Circular Substrates of the Hammerhead Ribozyme Shift the Internal Equilibrium Further toward Cleavage†

Tracy K. Stage-Zimmermann‡ and Olke C. Uhlenbeck*

Department of Chemistry and Biochemistry, University of Colorado, Boulder, Colorado 80309-0215

Received February 6, 1998; Revised Manuscript Received April 24, 1998

ABSTRACT: To test whether the Y-shaped conformation of the hammerhead ribozyme is maintained throughout the catalytic pathway, the cleavage properties of circular substrates which bind the ribozyme through helices I and II were determined. Constraining the position of helices I and II in this manner did not significantly alter the rate constant for cleavage, consistent with no large rearrangement of the helices occurring during catalysis. Unexpectedly, the "internal" equilibrium between the cleavage and ligation reactions for the circular hammerheads was shifted further toward cleavage. This effect was due to the rate of ligation of the circular substrate being slower than the corresponding linear substrate. The temperature dependence of the internal equilibrium of the circular substrate revealed that although restricting the flexibility of the hammerhead reduced the favorable entropy change associated with cleavage as expected, the unfavorable enthalpy change was reduced as well, resulting in greater overall cleavage.

The X-ray crystal structures of two different hammerhead ribozyme−inhibitor complexes revealed a global fold that resembles the letter Y (*1*, *2*). Unlike the original secondary structure representation, helices I and II are the closest in space, and helix III is nearly coaxially stacked on helix I. Several studies of inactive hammerhead ribozymes in solution have confirmed this Y conformation with only minor variations in the positioning of the three helices (*3*−*5*). It is not clear, however, whether this fold is maintained throughout the hammerhead cleavage reaction pathway. It has been known for many years that cleavage by the hammerhead ribozyme proceeds through in-line attack of the scissile phosphodiester bond by the attacking 2′-hydroxyl (*6*−*8*); however, these functional groups are not in the proper orientation for catalysis in either of the crystal structures (*1*, *2*). In addition, there is an abundance of biochemical data on functional group substitutions that are incompatible with the crystal structure (*9*). For example, recent experiments have suggested that a metal ion bound to a phosphate located nearly 20 Å away from the cleavage site in the X-ray crystal structures is essential for catalysis (*10*). The discrepancies between the biochemical results and structural data have led to the suggestion that a fairly large rearrangement of the hammerhead must occur prior to reaching the transition state for cleavage (*10*). Such a rearrangement could lead to a transient change in the Y-shaped hammerhead conformation.

Despite the fact that the enthalpy change for the hammerhead ribozyme favors ligation over cleavage, the cleavage rate constant is 100-fold faster than the ligation rate constant (*11*). This unusual feature of the hammerhead is due to a large positive entropy change that accompanies cleavage (*12*). It was suggested that this entropy change could in large part be due to an increase in the flexibility of the ribozyme−product complex (*12*). Such a motion could be as large as a global rearrangement of the three helices or as small as a repositioning of residues in the catalytic core. Gel electrophoretic mobility and transient electric birefringence experiments suggest that the global structure of the cleaved ribozyme−product complex is similar to that of the uncleaved complex (*3*, *13*), while NMR spectroscopy and time-resolved crystallography detected local rearrangements of the catalytic core upon cleavage (*14*, *15*). None of these methods, however, look directly at the ribozyme's structure throughout the transition state.

Because of the above considerations, the cleavage and ligation properties of a hammerhead ribozyme in which the orientation of helices I and II was constrained by ligating the 5′ and 3′ ends of the substrate were investigated. If helices I and II as seen in the crystal structure need to move during catalysis, then maintaining the hammerhead in its Y-shape conformation could prevent cleavage or reduce the rate of cleavage. If the flexibility of the ribozyme−product complex contributes to driving the reaction toward products and the lower rate of ligation, then restricting the motion of the cleaved hammerhead could increase the rate of ligation.

MATERIALS AND METHODS

RNA Synthesis. The substrate RNAs, Sα7, Sα7-A_2, and Sα7-A_5, were synthesized by in vitro transcription of synthetic DNA templates with T7 RNA polymerase and subsequently gel-purified on 20% acrylamide/7 M urea gels as described previously (*16*, *17*). The ribozyme (Rα7) and the circularly permuted substrate containing the U_5 linker ($^{5'}G_{16.4}$CGUCUAGCGCG**UUUUU**GGGAAUCGAAACGCGAAA$_{L3.4}{}^{3'}$) were chemically synthesized by standard phosphoramidite chemistry, deprotected (*18*), and gel-purified as described previously (*11*). The 3′ product RNA, P2α7,

† This work was supported by NIH Grant AI30242.

* To whom correspondence should be addressed.

‡ Current address: Department of Biological Chemistry and Molecular Pharmacology, Harvard Medical School and Department of Cancer Biology, Dana-Farber Cancer Institute, Boston, MA 02115.

S0006-2960(98)00307-9 CCC: $15.00
Published on Web 06/12/1998

was chemically synthesized and deprotected as described previously (*18*) with a few minor modifications. After the second deprotection step, the RNA was desalted using a high-capacity, reverse-phase (C_{18}) column (6 mL, Bakerbond spe). The RNA was gel-purified on a 20% polyacrylamide/7 M urea gel, eluted from the gel in 0.5 M NH_4OAc, 1 mM EDTA, and subsequently desalted on a C_{18} column.

Preparation of Circular Substrates. The 5′-triphosphate of transcribed substrate RNAs was removed by treatment with calf intestine alkaline phosphatase and subsequently 5′ end labeled with [γ-^{32}P]ATP and *Pse*T I kinase which lacks the 3′-phosphatase activity associated with T4 polynucleotide kinase (*19*). Typical conditions for a 10 μL kinase reaction were 1.2 μM S, 50 mM Hepes, pH 7.8, 10 mM $MgCl_2$, 0.1 mM spermidine, 5 mM DTT, 1.3 μM [γ-^{32}P]ATP, and 2 units of *Pse*T I kinase incubated for 1 h at 37 °C. The reaction was incubated at 95 °C for 2 min to heat-inactivate the *PseT* 1 kinase before proceeding with the ligation reaction. For the ligation, $MgCl_2$, Hepes, pH 7.8, DTT, ATP, DMSO, and T4 RNA ligase were added directly to the kinase mixture to give final concentrations of 10 mM $MgCl_2$, 50 mM Hepes, pH 7.8, 5 mM DTT, 50 μM ATP, 20% DMSO, and 4−6 units of T4 RNA ligase in 40 μL. The ligation reaction was incubated for 1.5 h at 37 °C, and 40 μL of 88% formamide, 50 mM EDTA, bromophenol blue, and xylene cyanol (stop solution) was added to stop the reaction. After heating the reaction for 2 min at 95 °C, the mix was loaded on a 10% Long Ranger/7 M urea/0.6× TBE gel (acrylamide derivative made by FMC Bioproducts). The ligated circular substrate migrates faster then the linear substrate in this gel. RNAs were eluted from the gel in 0.5 M NH_4OAc, 1 mM EDTA, precipitated directly from the eluant, and resuspended in dH_2O for use in cleavage reactions. The linear substrate RNAs used for the control reactions were 5′ end labeled as described above and purified directly on 15% acrylamide/7 M urea gels.

Production of Cleaved Circular RNA and P1α7>p. To generate the cleaved circular RNA (Scirc>p) containing the 2′,3′-cyclic phosphate and 5′-hydroxyl termini, purified circular substrate was cleaved with Rα7. Labeled circular S, 55.6 mM Hepes, pH 7.8, and 5.56 μM Rα7 were combined in 36 μL and heated at 95 °C for 1.5 min, cooled to room temperature for at least 10 min, and incubated at 25 °C. To initiate cleavage, 4 μL of 0.1 M $MgCl_2$ was added, and the reaction was incubated for 1 h at 25 °C. The cleavage reaction was quenched by addition of 40 μL of stop solution, heated at 95 °C for 2 min, and purified as described above on a 10% Long Ranger/7 M urea/0.6× TBE gel.

For production of the 5′ product, P1α7>p, Sα7 was 5′ end labeled with *PseT* 1 kinase as described, and the RNA was precipitated directly from the kinase reaction. The labeled substrate was resuspended in 25 μL of dH_2O and cleaved by Rα7 as described for the circular substrate. ^{32}pP1α7>p was separated from ^{32}pSα7 on a 15% acrylamide/7 M urea gel and eluted from the gel as described for the circular substrate.

Measurement of k_2. 2.2, 5.6, or 10.9 μM Rα7, trace 5′ end labeled substrate (<1 nM ^{32}pS), and 55 mM Pipes, pH 7, were combined in 21.6 μL and heated at 95 °C for 1.5 min, cooled to room temperature for at least 10 min and then incubated at the reaction temperature. For the zero time point, 1.8 μL of the reaction mix was removed and added to 10 μL of stop solution. The reaction was initiated by adding 2.2 μL of 0.1 M $MgCl_2$, and 2 μL aliquots were removed at various times and quenched in 10 μL of stop solution. Final reaction conditions were 2, 5, or 10 μM Rα7, trace ^{32}pS, 50 mM Pipes, pH 7, and 10 mM $MgCl_2$. Substrate and products were separated either on a 15% polyacrylamide/7 M urea gel for the linear substrates or on a 10% Long Ranger/7 M urea/0.6× TBE gel for the circular substrates. The fraction product was quantitated using a Molecular Dynamics Phosphorimager.

Measurement of the Rate of Approach to Equilibrium (k_{app}) and Calculation of k_{-2}. The rate of approach to equilibrium was measured from the reverse direction. For the circular substrates, 5.6 μM Rα7, trace ^{32}pSα7-A_5circ>p, and 100 mM Pipes, pH 6.5, were combined in 21.6 μL, heated at 95 °C for 1.5 min, cooled to room temperature, and then placed in a 10 °C water bath. For time zero, 1.8 μL of the reaction mix was removed and put in 20 μL of stop solution on ice. To start the reaction, 2.2 μL of precooled 1 M $MgCl_2$ in 0.1 M Pipes, pH 6.5, was added to the mix. The final reaction conditions were 5 μM Rα7, trace ^{32}pSα7-A_5circ>p, 100 mM Pipes, pH 6.5, and 100 mM $MgCl_2$ at 10 °C. Eight 2 μL aliquots were taken at specific times and quenched in 20 μL of stop solution on ice. The ligated circle was separated from the cleaved circle on a 25% acrylamide/7 M urea/0.5× TBE gel where the linear RNA migrates faster. The reaction was carried out in the same manner for the linear control except that both ^{32}pP1α7>p and P2α10 were required for the reaction. The final conditions for the linear control were 5 μM Rα7, trace ^{32}pP1α7>p, 10 μM P2α7, 100 mM Pipes, pH 6.5, and 100 mM $MgCl_2$ at 10 °C. The ligated substrate was separated from the cleaved product on a 15% acrylamide/7 M urea gel where the ligated substrate migrated slower than ^{32}pP1α7>p. For both the circular and linear RNAs, the fraction ligated substrate was quantitated, plotted as a function of time, and fit to eq 1, where k is equal to k_{app}. The rate of ligation, k_{-2}, was

$$\frac{S}{S+P} = \left(\frac{S}{S+P}\right)_0 + \left(\frac{S}{S+P}\right)_\infty (1 - e^{-kt}) \qquad (1)$$

calculated from eq 2:

$$k_{-2} = \frac{(1/K_{eq}^{Int})k_{app}}{1 + 1/K_{eq}^{Int}} \qquad (2)$$

using the rate of approach to equilibrium, k_{app}, and the ratio of substrate to product at equilibrium, $1/K_{eq}^{Int}$, as determined from the above experiment.

Measurement of $1/K_{eq}^{Int}$. The reaction conditions for measuring the temperature dependence of $1/K_{eq}^{Int}$ were similar to those described previously (*12*, *20*). For the circular RNAs, 5.6 μM Rα7, trace ^{32}pScirc>p, and 100 mM Pipes, pH 6.5, were combined in 81 μL, heated at 95 °C for 2 min, and then cooled to room temperature for at least 15 min. Nine microliters of 1 M $MgCl_2$ in 0.1 M Pipes, pH 6.5, was added to the mix, and the mixture was divided into seven 12 μL aliquots. Each aliquot was layered with approximately 5 μL of mineral oil to prevent the buildup of condensation during the time of incubation, and each reaction was placed at a different temperature, ranging from 4 to 37 °C for 12−24 h. Multiple time points were taken to verify that the

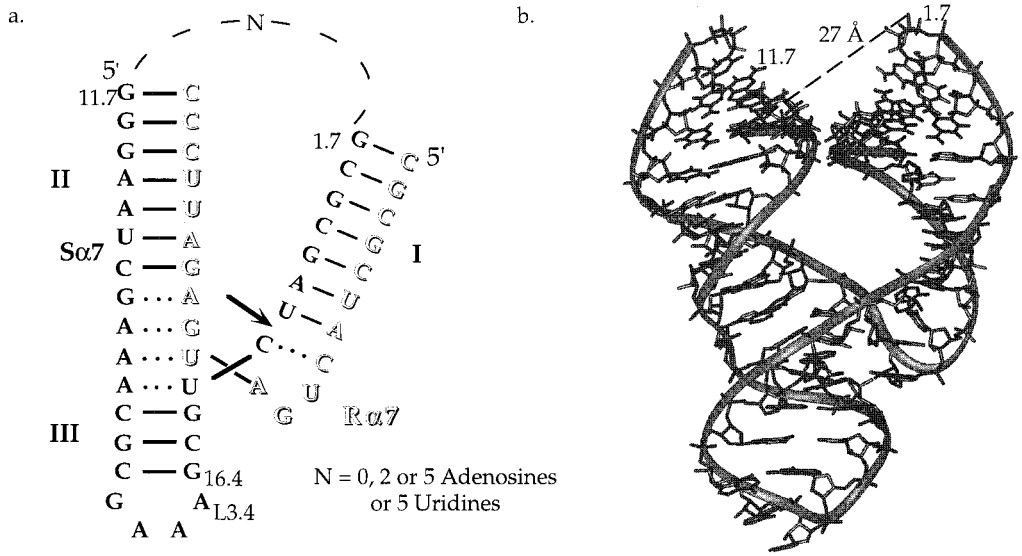

FIGURE 1: (A) Schematic representation of HHα7 based on the three-dimensional structure of the hammerhead ribozyme. The dotted line between residues 1.7 and 11.7 of the substrate represents the linker between the two ends of the substrate when ligated to form a circle. The arrow represents the site of cleavage, 3′ of C_{17}. Residues 16.4 and L3.4 are the 5′ and 3′ ends of the circularly permuted substrate containing five uridines in the linker. (B) Three-dimensional model of the hammerhead ribozyme with two and three additional base pairs modeled onto the ends of helix I and II, respectively. The distance marked is between the phosphate of residue 11.7 and the O3′ of residue 1.7.

reaction was at equilibrium. Typically, three 3 μL aliquots were removed at time intervals of 1−2 h apart and quenched in 40 μL of 88% formamide, 50 mM EDTA, bromophenol blue, and xylene cyanol on ice. The ligated circular substrate was separated from the cleaved circle on a 25% acrylamide/7 M urea/0.5× TBE gel. The ratio of ligated circle to cleaved circle (*S*/*P*) was quantitated using a Molecular Dynamics Phosphorimager, plotted as a function of temperature, and fit directly to the van't Hoff equation. The protocol for the linear control was similar to the circular RNAs with the only difference being the input RNAs. The final conditions for the linear control were 5 μM Rα7, trace ^{32}pP1α7>p, 10 μM P2α7, 100 mM Pipes, pH 6.5, and 100 mM $MgCl_2$. The ligated substrate was separated from ^{32}pP1α7>p on a 15% acrylamide/7 M urea gel and quantitated as described above. The values of *S*/*P* for the linear A_5 and circular A_5 hammerheads plotted in Figure 4 are from three separate equilibrium experiments. The values of *S*/*P* for the circular U_5 hammerhead are three end points taken from the same reaction. The errors reported for $\Delta H°$ and $\Delta S°$ are the standard error values determined by the curve-fitting program (Kaleidagraph 3.0) with an allowable error of 0.1%.

Measurement of the Magnesium Ion Dependence of 1/K_{eq}^{Int}. The reactions were set up in the same manner as described for the temperature dependence of $1/K_{eq}^{Int}$ except that the concentration of $MgCl_2$ used to initiate the reaction varied from 5 M down to 7.8 mM, resulting in reactions that contained 0.5 M to 0.78 mM $MgCl_2$. The $MgCl_2$ stock solutions were serially diluted with 0.1 M Pipes, pH 6.5, starting at 5 M $MgCl_2$ in 0.1 M Pipes, pH 6.5. The reactions were incubated at 10 °C, and at least three, 3 μL time points were taken and quenched in 40 μL of 88% formamide, 0.1 M EDTA, xylene cyanol, and bromophenol blue, on ice. The ratio of ligated substrate to cleaved product at equilibrium from three separate experiments was plotted as a function of $MgCl_2$ concentration for both the linear A_5 and circular A_5 hammerheads and fit to a hyperbolic binding equation to obtain K_p and $1/K_{eq}^{Int,sat}$ as described previously (*20*). The errors reported for K_p and $1/K_{eq}^{Int,sat}$ are the standard error values derived from the curve-fitting program with an allowable error of 0.1%.

RESULTS

The hammerhead ribozyme used in this study (HHα7) is similar to the sequence of a well-characterized I/II format hammerhead (HHα1) (*21*) with two additional base pairs at the ends of helix I and helix II (Figure 1A). The extra base pairs were added to increase the affinity of the products to the ribozyme such that the reverse reaction could be measured (*11*). To restrain helices I and II, the 5′ and 3′ ends of the substrate strand were ligated with or without an intervening linker to make circular substrates for the ribozyme (Figure 1A). To estimate the distance between the 5′ and 3′ ends of the substrate strand when bound to the ribozyme, two and three base pair helical extensions were modeled onto the ends of helices I and II of the X-ray crystal structure (Figure 1B) (*2*). The distance between the phosphate of residue 11.7 at the end of helix II and O3′ of residue 1.7 at the end of helix I was 27 Å. Based on this information, three different linker lengths were chosen, zero (A_0), two (A_2), or five adenosines (A_5). A linker containing five uridines was also prepared to test whether the composition of the linker was important. The rationale for choosing the linker lengths was that five nucleotides should easily span the gap between the two stems, given that the phosphate to phosphate distance should be about 5.9 Å (*22*), whereas zero or two nucleotides should shorten the distance and possibly decrease the angle between the two helices. All of the linkers should restrict the hammerhead from any major reorientation of the helices. It is possible that the shorter linkers could cause the ends of either helix to fray in order to maintain the crystal structure conformation. To maintain the distance between the two helices, three or five base pairs would need to be disrupted to span the 27 Å gap for the two or zero adenosine linkers, respectively. Since a base pair typically contributes 1−2 kcal/mol to the energy of binding (*23*, *24*),

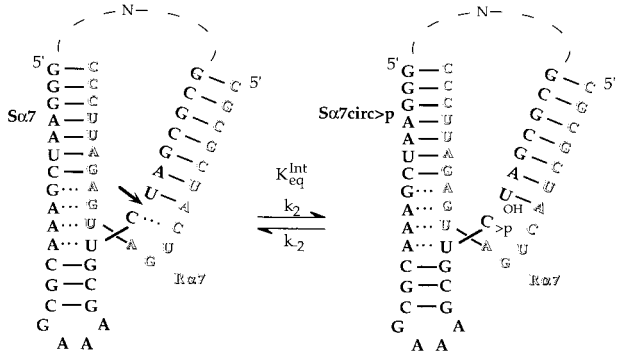

FIGURE 2: Schematic of the cleavage step for a circular substrate. Rα7 is the ribozyme; Sα7 is the substrate which has 0, 2, or 5 adenosines, or 5 uridines as its linker between the two helices; and Sα7circ>p is the cleaved circular substrate containing a 2′,3′-cyclic phosphate at its 3′ end and a 5′-hydroxyl at its 5′ end. The cleavage site is marked by an arrow. k_2 is the rate of cleavage, k_{-2} is the rate of ligation, and $K_{eq}^{Int} = k_2/k_{-2}$. The entire kinetic pathway (*25*) is not depicted since the substrate binding and product release steps were not investigated.

Table 1: k_2 for Linear and Circular Substrates of HHα7

hammerhead	k_2 (min^{-1})[a,b] (10 mM $MgCl_2$)	k_2 (min^{-1})[c] (0.5 mM $MgCl_2$)	k_2 (min^{-1})[c] (2 mM $MgCl_2$)
HHα7 linear A_0	0.79 ± 0.02		
HHα7 circular A_0	1.2 ± 0.1		
HHα7 linear A_2	0.70 ± 0.04		
HHα7 circular A_2	0.35 ± 0.01		
HHα7 linear A_5	0.72 ± 0.01	0.22 ± 0.03	1.3 ± 0.05
HHα7 circular A_5	0.23 ± 0.01	0.23 ± 0.01	0.51 ± 0.02
HHα7 linear U_5	0.39 ± 0.01		
HHα7 circular U_5	0.34 ± 0.01		

[a] Rates were determined at pH 7 and 25 °C. [b] The k_2 values reported are the average of at least three independent experiments with the standard deviation reported as the error. [c] Rates were determined at pH 7.5, 25 °C. Error values were derived by the curve-fitting program given an allowable error of 0.1%.

this type of fraying would be expected to weaken the binding of the substrate to the ribozyme significantly.

The substrate RNAs either containing adenosines in the linker or having no linker were transcribed off of synthetic DNA templates using T7 RNA polymerase and purified as described previously (*25*). After dephosphorylation of the 5′-triphosphate and 5′ end labeling the RNA with [γ-^{32}P]-ATP, the two ends of the RNA were ligated using T4 RNA ligase (*26*). The circular substrate RNA was separated from the linear input RNA by denaturing gel electrophoresis and isolated for use in cleavage assays. Because T4 RNA ligase does not ligate efficiently when uridine is the acceptor (*26*), the substrate with five uridines in the linker was made by preparing a circularly permuted version of the substrate. The 5′ end of the substrate RNA was placed at guanosine 16.4 in stem III and the RNA terminated with an adenosine at position L3.4 (Figure 1A). The uridines that make up the linker were therefore in the middle of the full-length RNA. The preparation of the circular U_5 substrate was otherwise similar to the adenosine linker substrates.

The rate of chemistry, k_2, for the circular substrates was compared to that of the linear control substrates (Figure 2). A saturating amount of ribozyme was used to ensure that the rate-limiting step of the reaction was the cleavage step. Table 1 summarizes the k_2 values for both the circular and linear substrates measured at pH 7, 10 mM $MgCl_2$, and 25 °C. All of the circular substrates cleaved at rates within 3-fold of their respective linear control substrates. The largest difference in k_2 was a 3-fold reduction for the A_5 circular substrate. Lowering the magnesium chloride concentration to either 0.5 or 2 mM had little effect on the difference in k_2 measured for the A_5 circular and linear substrates (Table 1).

Experiments were carried out to confirm that the rate of cleavage for the circular and linear substrates reflected the rate of the chemical step (k_2). More than one high ribozyme concentration gave the same rate, and similar ribozyme concentrations achieved saturation for all of the substrates, indicating that binding was not rate-limiting under the conditions of this assay. The rates of cleavage for all of the substrates were pH-dependent by the expected amount (*12*, *27*) which is indicative of the rate of chemistry being measured. Finally, the kinetics of cleavage were first order for all of the substrates, and the extent of cleavage was greater than 80%, consistent with the substrate folding properly.

The rate of approach to equilibrium ($k_{app} = k_2 + k_{-2}$) measured from either the forward or the reverse direction is dominated by k_2 which is much faster than k_{-2} for the hammerhead ribozyme (*11*). Therefore, if the reaction pathway has not been greatly altered for the circular substrates, the rate of approach to equilibrium from the reverse direction should also be close to k_2. To test this prediction, k_{app} was measured from the reverse direction for the circular A_5 hammerhead and compared to that of the linear A_5 hammerhead. The reaction is set up in a manner similar to the k_2 measurement but starts with the cleaved product oligonucleotide(s). For the circular substrates, the product is a linear RNA having a 2′,3′-cyclic phosphate (>p) at its 3′ end and a hydroxyl at its 5′ end (Sα7circ>p) (Figure 2). The linear control has two products, the 5′ product with a 2′,3′-cyclic phosphate (P1α7>P) and the 3′ product with a 5′-hydroxyl (P2α7). For the circular RNAs, a saturating concentration of ribozyme was used to ensure that every labeled product was bound to a ribozyme. The same ribozyme concentration was used for the linear control with trace 5′ end labeled P1α7>p and 2-fold excess P2α7 over the ribozyme concentration, such that any ribozyme with a bound 5′ product also had a bound 3′ product. The reaction was initiated by the addition of $MgCl_2$, and time points were taken up to and including the end point (equilibrium) of the reaction. Since it has been shown for other hammerheads that the extent of ligation is greater at low temperatures and high magnesium ion concentrations (*12*, *20*), 10 °C, 100 mM $MgCl_2$, and pH 6.5 were the conditions chosen for this experiment. A plot of the fraction ligated substrate ($S/S + P$) as a function of time was fit to a single exponential to obtain k_{app} (Figure 3). In parallel, k_2 was determined under the same reaction conditions. As seen clearly in Figure 3, the extent of ligation for the circular RNA is greatly reduced from that of the linear control. However, the rate of approach to equilibrium (k_{app}) is essentially the same as k_2 for both the linear and circular A_5 substrates (Table 2). The rate of ligation, k_{-2}, was also calculated from this experiment (Table 2). Both the rate of cleavage and the rate of ligation are slightly reduced for the circular hammerhead relative to the linear control. k_2 was 3-fold slower for the circular A_5 substrate as compared to the linear control (Table 2), similar

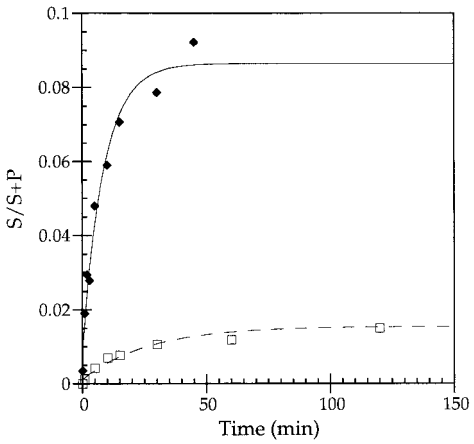

FIGURE 3: Rate of approach to equilibrium, k_{app}. Plot of the fraction of substrate ligated as a function of time measured at pH 6.5, 10 °C, and 100 mM $MgCl_2$ for the linear A_5 (◆) and circular A_5 (□) hammerheads. The data are fit to $S/(S + P) = [S/(S + P)]_0 + [S/(S + P)]_\infty(1 - e^{-k_{app}t})$, giving k_{app} of 0.11 min^{-1} for the linear A_5 hammerhead and 0.03 min^{-1} for the circular A_5 hammerhead.

Table 2: k_2, k_{app}, and k_{-2} for Linear and Circular A_5 Hammerheads

hammerhead	k_2 $(min^{-1})^{a,b}$	k_{app} $(min^{-1})^{a,b}$	k_{-2} $(min^{-1})^{c}$	$K_{eq}^{Int\,d}$
HHα7 linear A_5	0.14 ± 0.03	0.11 ± 0.01	0.009	16
HHα7 circular A_5	0.04 ± 0.01	0.03 ± 0.01	0.0005	80

[a] Rates were determined at pH 6.5, 100 mM $MgCl_2$, and 10 °C. [b] The rates reported are the average of at least three independent experiments with the standard deviation reported as the error. [c] Calculated from experimentally determined k_{app} and $1/K_{eq}^{Int}$; see Materials and Methods. [d] Calculated from the relationship: $K_{eq}^{Int} = k_2/k_{-2}$.

to the difference observed at higher temperature and at a lower magnesium concentration (Table 1). In contrast, k_{-2} is reduced by a much greater extent (18-fold) for the circular hammerhead which results in a change in the internal equilibrium ($K_{eq}^{Int} = k_2/k_{-2}$) from 16 for the linear A_5 hammerhead to 80 for the circular A_5 hammerhead (Table 2).

To determine the thermodynamic properties of the internal equilibrium for the circular substrates, this constant was measured as a function of temperature to obtain the change in entropy ($\Delta S°$) and enthalpy ($\Delta H°$) for the reaction. The equilibrium was approached from the reverse direction under similar conditions to the previous experiment. The reactions were placed at several temperatures ranging from 4 to 37 °C and incubated for 12−24 h to make sure that each reaction had reached equilibrium. The ratio of ligated substrate to cleaved product at equilibrium ($S/P = 1/K_{eq}^{Int}$) was quantitated, plotted as a function of temperature in Kelvin, and fit to the van't Hoff equation to obtain the thermodynamic parameters $\Delta H°$ and $\Delta S°$.

Figure 4 shows representative data for the linear A_5, circular A_5, and circular U_5 hammerheads. As seen from this plot, the ratio of ligated substrate to cleaved product (S/P) increases at lower temperatures for the circular hammerheads but to a much lower extent than the linear control. Thus, cleavage is even more favored over ligation for the circular hammerheads. The profile for the linear A_5 hammerhead is similar to that previously determined for other unmodified hammerheads (*12*, *20*), increasing up to 0.16 S/P at 4 °C. The profiles for both the circular A_5 and U_5 hammerheads are similar to each other in shape; however, the amount of ligated circular substrate for the U_5 hammerhead is greater by a similar amount at each temperature. At both 30 and 37 °C, the ratio of substrate to product for the circular U_5 hammerhead overlays with that of the linear A_5 hammerhead; however, at lower temperatures, this ratio is decreased relative to the linear control. The data for the A_2 circular hammerhead were similar to both the A_5 and U_5 circular RNAs except for lower overall extents of ligation at each temperature (data not shown). Ligated substrate for the circular RNA without a linker was not observed at the limit of detection for this assay of 0.1% ligation. Since S/P for the A_2 circular hammerhead was already very low, it is possible that ligation of the circular A_0 RNA occurred but that it could not be resolved from the background. Alternatively, the ribozyme may not be able to form the proper conformation with the cleaved A_0 circle to catalyze ligation.

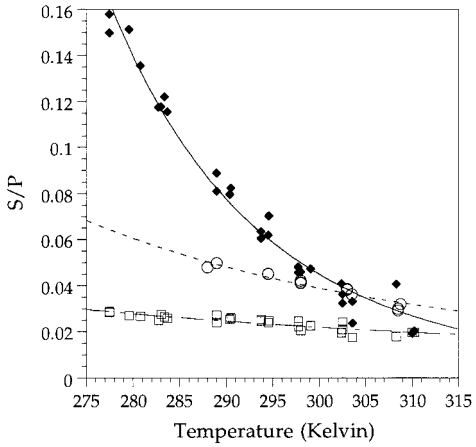

FIGURE 4: Temperature dependence of $1/K_{eq}^{Int}$. Plot of the ratio of ligated substrate to cleaved product ($1/K_{eq}^{Int}$) as a function of temperature in Kelvin for the linear A_5 (◆), circular A_5 (□), and circular U_5 (○) hammerheads. The data were fit directly to the van't Hoff equation: $1/K_{eq}^{Int} = \exp(-\Delta H°/RT + \Delta S°/R)$, where R is the gas constant [0.00198 (*kcal*/*mol* × *K*)], T is the temperature in Kelvin, $\Delta H°$ is the change in enthalpy, and $\Delta S°$ is the change in entropy. The $\Delta H°$ and $\Delta S°$ for each hammerhead are summarized in Table 3.

The lower extents of ligation for the circular hammerheads were not due to hydrolysis of the 2′,3′-cyclic phosphate at the 3′ end of the cleaved product RNA during its workup. The presence of the 2′,3′-cyclic phosphate was confirmed by P1 nuclease digestion of [α-^{32}P]UTP-labeled, cleaved circular A_5 substrate and subsequent analysis by thin-layer chromatography (TLC) as described previously (*28*). As predicted from the sequence of the RNA, only ^{32}pU and pC>^{32}p were present for the cleaved circular RNA. pC^{32}p, the breakdown product of pC>^{32}p, was not detected.

The thermodynamic parameters, $\Delta H°$ and $\Delta S°$, for the forward equilibrium ($K_{eq}^{Int} = k_2/k_{-2}$) are summarized in Table 3 for the linear and circular substrates of HHα7. $\Delta H°$ and $\Delta S°$ for the linear substrates with zero or five dangling adenosines at the 3′ end are very similar to those reported previously for both an intermolecular and an intramolecular hammerhead (*12*, *20*). Since no significant differences resulted from having zero or five dangling adenosines at the 3′ end of the linear substrate RNAs, the enthalpy and entropy changes were not determined for the A_2 or U_5 linear substrates. The $\Delta S°$ and $\Delta H°$ for the circular A_2 and circular A_5 hammerheads were essentially identical, and both $\Delta S°$ and $\Delta H°$ decreased relative to the linear controls. $\Delta S°$ was

Table 3: Thermodynamic Parameters for the Linear and Circular Substrates of HHα7

hammerhead	$\Delta H°$ [b] (kcal/mol)	$\Delta S°$ [b] (eu)	$\Delta G°_{283}$ [c] (kcal/mol)
HHα7 linear A_0	8.8 ± 0.5	36 ± 2	−1.4
HHα7 circular A_0[a]	ND	ND	ND
HHα7 circular A_2	1.4 ± 0.2	12.9 ± 0.5	−2.3
HHα7 linear A_5	9.5 ± 0.3	38 ± 1.0	−1.3
HHα7 circular A_5	1.9 ± 0.2	14 ± 1.0	−2.1
HHα7 circular U_5	3.7 ± 0.3	19 ± 1.0	−2.0

[a] ND = no ligation detected. [b] $\Delta H°$ and $\Delta S°$ are for the forward equilibrium (K_{eq}^{Int}). The errors reported are the standard error values derived by the curve fitting program given an allowable error of 0.1%. [c] $\Delta G°$ at 10 °C was calculated from the relationship: $\Delta G° = \Delta H° - T\Delta S°$.

reduced from ~38 eu for the linear controls to ~14 eu for the circular hammerheads, and $\Delta H°$ was reduced from ~9 kcal/mol to ~1.5 kcal/mol, respectively. Both the enthalpy and entropy for the circular U_5 hammerhead were slightly higher than the circular A_2 and A_5 hammerheads, giving a $\Delta S°$ of 19 eu and a $\Delta H°$ of +3.7 kcal/mol. Although the entropy change was decreased for all of the circular hammerheads, the reaction still favored cleavage because the unfavorable enthalpy change associated with cleavage was also reduced. The calculated free energy difference at 10 °C for the forward equilibrium demonstrates that cleavage of the circular substrates is favored by 0.6−1 kcal/mol over the linear substrates at this temperature (Table 3).

It was previously suggested that metal ion dissociation from the enzyme product complex contributes to driving the hammerhead cleavage reaction toward product formation (*20*). To investigate whether the apparent metal ion affinity had changed for the circular hammerheads, the $MgCl_2$ dependence of the internal equilibrium was measured for both the circular and linear A_5 hammerheads. The ratio of ligated substrate to cleaved product for both hammerheads was measured at pH 6.5, 10 °C, and several $MgCl_2$ concentrations ranging from 0.78 mM to 0.5 M. Figure 5 is a plot of *S*/*P* as a function of $MgCl_2$ concentration fit to a hyperbolic binding equation to obtain the apparent magnesium ion binding constant for the internal equilibrium (K_p) and the equilibrium at saturating metal ion concentration ($1/K_{eq}^{Int,sat}$). K_p for the circular A_5 hammerhead was 42 ± 4 mM, 3-fold higher than K_p of 13 ± 1 mM for the linear A_5 hammerhead. The values for $1/K_{eq}^{Int,sat}$ were 0.044 for the circular A_5 hammerhead and 0.14 for the linear A_5 hammerhead. Thus, even at saturating metal ion concentrations, the circular hammerhead favors cleavage more than the linear hammerhead. Both the K_p and $1/K_{eq}^{Int,sat}$ for the linear A_5 hammerhead were similar to values previously measured for both an intermolecular and an intramolecular hammerhead (*12*, *20*).

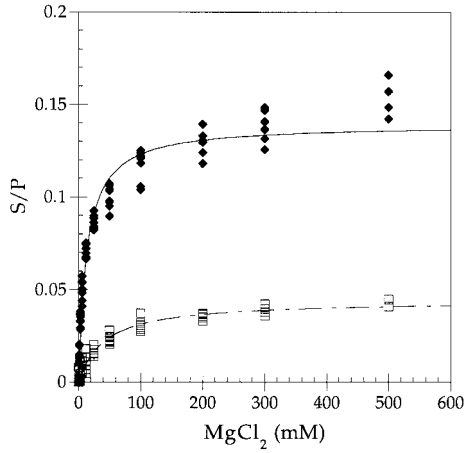

FIGURE 5: Magnesium dependence of $1/K_{eq}^{Int}$. Plot of the ratio of ligated substrate to cleaved product ($1/K_{eq}^{Int}$) as a function of magnesium chloride concentration for the linear A_5 (◆), and circular A_5 (□) hammerheads. The data were fit to $1/K_{eq}^{Int} = [M/(K_p + M)] \times (1/K_{eq}^{Int,sat})$ where M is the magnesium concentration, K_p is the apparent metal ion dissociation constant, and $1/K_{eq}^{Int,sat}$ is the equilibrium constant at saturating magnesium. For the linear A_5 hammerhead, K_p is 13 ± 1 mM and $1/K_{eq}^{Int,sat}$ is 0.14; and for the circular A_5 hammerhead, K_p is 42 ± 4 mM and $1/K_{eq}^{Int,sat}$ is 0.044.

DISCUSSION

Only small changes in the rate of chemistry, k_2, occurred upon circularizing the substrate (Table 1). All of these k_2 effects are small in terms of the transition state barrier for cleavage by the hammerhead ribozyme (*12*). Therefore, our results suggest that a gross change of the orientation of the three helices of the hammerhead ribozyme is not required during cleavage and that the conformational constraint imposed by circularizing the substrate does not interfere with any structural rearrangements that are needed for catalysis to occur. For example, the repositioning of any core nucleotides that may be required for cleavage must be able to occur with helices I and II linked. A similar conclusion can be reached from the observation that an intramolecular disulfide cross-link between helices I and II of the ribozyme strand had no effect on the rate of the forward reaction (*29*).

It was demonstrated previously that the orientation of helices I, II, and III, as determined by a gel mobility assay, changes as a function of magnesium ion concentration (*5*). At low magnesium concentrations (0.5 mM) where the hammerhead is less active, the ribozyme resembles the original secondary structure representation with helices I and II forming the base of an upside-down T. Based on this and other data, it was hypothesized that a switch from the upside-down T conformation to the active Y conformation is required for cleavage to occur (*5*, *30*). If this conformational switch influences the rate of the chemical step in solution, it may be expected that the rate of cleavage for a circular substrate, which holds the hammerhead in the Y conformation, would be faster at low $MgCl_2$ concentrations. A rate enhancement was not observed for the circular A_5 substrate at low $MgCl_2$ concentrations (Table 1). These data suggest that if the conformational switch observed by gel electrophoresis occurs in solution, it is fast relative to cleavage.

The rate of approach to equilibrium from the reverse direction (k_{rev}) was dominated by the rate of cleavage (k_2) for the circular A_5 substrate (Table 2), indicating that it has the same rate-limiting step as does the linear substrate. Surprisingly, the extent of ligation was dramatically reduced for the circular A_5 RNA (Figure 3). At 10 °C, the internal equilibrium for the circular substrate actually favors cleavage 80-fold over ligation as compared to only 16-fold for the linear substrate (Table 2). The shift in equilibrium further toward product formation was due to a decrease in the rate of ligation (k_{-2}) for the circular A_5 hammerhead at this

temperature (Table 2). This result is opposite to the expectation that reducing the motions of the enzyme−product complex (E·P) by constraining helices I and II would shift the equilibrium toward ligation by increasing the rate of the reverse reaction.

The thermodynamic analysis of the equilibrium helps to understand why cleavage is favored even more for the circular hammerhead. Although the change in entropy upon cleavage was reduced from 38 eu for the linear hammerhead to 14 eu for the circular hammerhead, product formation was still favored because the unfavorable enthalpy change associated with cleavage also decreased from +9 kcal/mol to +1.5 kcal/mol (Table 3). Changes in the entropy and enthalpy for the internal equilibrium reflect relative differences between the ribozyme−substrate (E·S) and ribozyme−product complexes (E·P). These differences can be variations in structure, motion, solvation, metal ion binding properties, or any other feature of the RNA that differs between the cleaved and uncleaved complexes (*12*, *20*). It is reasonable that at least a portion of the large decrease in $\Delta S°$ is the result of the conformational constraint introduced by linking the 5′ and 3′ ends of the substrate. Although this constraint is likely to reduce the molecular motions of both E·S and E·P when compared to the unconstrained hammerhead, it is reasonable to expect that the effect will be much greater for E·P since breakage of the phosphodiester bond at the cleavage site normally permits the hammerhead to sample additional degrees of freedom. Thus, the observed decrease in $\Delta S°$ is consistent with the original expectation that linking helices I and II would reduce the flexibility of E·P relative to an unrestricted hammerhead.

The source of the much smaller enthalpy change for the circular hammerheads is difficult to understand. Previously, the enthalpy change associated with cleavage by the hammerhead was attributed mostly to the 8 kcal/mol difference in $\Delta H°$ between the 3′,5′-phosphodiester of the substrate and 2′,3′-cyclic phosphate of the product (*12*). Since the termini of the cleaved circular substrate are the same, another source for the much smaller $\Delta H°$ of 1.5 kcal/mol must be sought. One possibility is that the linker nucleotides stack differently at the ends of the helices in the uncleaved versus cleaved complexes for the circular hammerheads; another is that the linker induces fraying of base pairs at the end of helix I or helix II in one but not the other complex. Changing the linker nucleotide to uridine, which does not stack as well as adenosine (*22*), only had a small effect on the enthalpy change (Table 3), suggesting that the identity of the linker is only a minor contributor to the enthalpy change for the circular hammerheads. Fraying is also not a likely explanation since the A_2 linker, which would be more likely to cause fraying of one of the two helices, had identical thermodynamic parameters as the A_5 linker, suggesting that this was not the source of the change in enthalpy either.

The magnesium dependence of the internal equilibrium provides a partial explanation for why the circular hammerheads may favor cleavage even more so than ligation. Long and co-workers proposed that upon cleavage a metal ion or ions dissociate from E·P and that this dissociation event contributes to driving the equilibrium toward cleavage (*20*). Increasing the metal ion concentration increases the population of E·P bound with metal and thus increases the extent of ligation at equilibrium. The apparent metal ion binding affinity (K_p) for the circular A_5 hammerhead was 3-fold weaker than for the linear A_5 hammerhead (Figure 5). This result is consistent with metal ion(s) dissociation from E·P occurring more readily for the circular hammerhead and thus driving the equilibrium further toward cleavage. This difference in metal ion binding cannot be the sole reason for the equilibrium shift for the circular hammerheads. At saturating metal ion concentrations, the equilibrium between ligated substrate and cleaved product ($1/K_{eq}^{Int,sat}$) for the circular A_5 hammerhead was still 3-fold lower than that of the linear A_5 hammerhead (Figure 5). Because metal ion binding is known to have both enthalpic and entropic components (*20*), the change in K_p for the circular hammerhead may have affected either $\Delta H°$ or $\Delta S°$. Thus, it appears that many factors including differences in structure and metal ion binding contributed to shifting the internal equilibrium further toward cleavage for the circular substrates.

The positive strand of the satellite RNA associated with barley yellow dwarf virus (sBYDV) contains a hammerhead-like motif that forms a stable pseudoknot between helices I and II that would also be expected to reduce its molecular motions (*31*, *32*). Unlike the circular substrates and disulfide cross-linked hammerhead (*29*) that did not affect cleavage, this naturally occurring link between helices I and II reduces the rate of self-cleavage by greater than 1000-fold. Self-cleavage of the sBYDV hammerhead is rescued upon disruption of this pseudoknot structure (*31*). The slow rate of cleavage of this sequence could be due to the pseudoknot twisting helices I and II of the hammerhead motif into a less active conformation, or alternatively the sBYDV hammerhead may have an altered internal equilibrium which favors ligation over cleavage. It has also been suggested that the pseudoknot may simply act as a switch between self-cleavage and some other function of the satellite RNA such as replication (*31*). Determining which of these roles the pseudoknot serves would be interesting to investigate further.

ACKNOWLEDGMENT

We thank Grant R. Zimmermann for modeling the helical extensions onto the ends of stems I and II of the X-ray crystal structure of the hammerhead ribozyme.

REFERENCES

1. Pley, H. W., Flaherty, K. M., and McKay, D. B. (1994) *Nature 372*, 68−74.
2. Scott, W. G., Finch, J. T., and Klug, A. (1995) *Cell 81*, 991−1002.
3. Amiri, K. M. A., and Hagerman, P. J. (1994) *Biochemistry 33*, 13172−13177.
4. Tuschl, T., Gohlke, C., Jovin, T. M., Westhof, E., and Eckstein, F. (1994) *Science 266*, 785−789.
5. Bassi, G. S., Møllegaard, N.-E., Murchie, A. I. H., von Kitzing, E., and Lilley, D. M. J. (1995) *Nat. Struct. Biol. 2*, 45−55.
6. van Tol, H., Buzayan, J. M., Feldstein, P. A., Eckstein, F., and Bruening, G. (1990) *Nucleic Acids Res. 18*, 1971−1975.
7. Koizumi, M., and Ohtsuka, E. (1991) *Biochemistry 30*, 5145−5150.
8. Slim, G., and Gait, M. J. (1991) *Nucleic Acids Res. 19*, 1183−1188.
9. McKay, D. B. (1996) *RNA 2*, 395−403.
10. Peracchi, A., Beigelman, L., Scott, E. C., Uhlenbeck, O. C., and Herschlag, D. (1997) *J. Biol. Chem. 272*, 26822−26826.
11. Hertel, K. J., Herschlag, D., and Uhlenbeck, O. C. (1994) *Biochemistry 33*, 3374−3385.

12. Hertel, K. J., and Uhlenbeck, O. C. (1995) *Biochemistry 34*, 1744−1749.
13. Amiri, K. M. A., and Hagerman, P. J. (1996) *J. Mol. Biol. 261*, 125−134.
14. Scott, W. G., Murray, J. B., Arnold, J. R. P., Stoddard, B. L., and Klug, A. (1996) *Science 274*, 2065−2069.
15. Simorre, J.-P., Legault, P., Hangar, A. B., Michiels, P., and Pardi, A. (1997) *Biochemistry 36*, 518−525.
16. Milligan, J. F., and Uhlenbeck, O. C. (1989) *Methods Enzymol. 180*, 51−62.
17. Fedor, M. J., and Uhlenbeck, O. C. (1990) *Proc. Natl. Acad. Sci. U.S.A. 87*, 1668−1672.
18. Wincott, F., DiRenzo, A., Shaffer, C., Grimm, S., Tracz, D., Workman, C., Sweedler, D., Gonzalez, C., Scaringe, S., and Usman, N. (1995) *Nucleic Acids Res. 23*, 2677−2684.
19. Cameron, V., Soltis, D., and Uhlenbeck, O. C. (1978) *Nucleic Acids Res. 5*, 825−833.
20. Long, D. M., LaRiviere, F. J., and Uhlenbeck, O. C. (1995) *Biochemistry 34*, 14435−14440.
21. Clouet-d'Orval, B., and Uhlenbeck, O. C. (1996) *RNA 2*, 483−491.
22. Saenger, W. (1984) *Principles of Nucleic Acid Structure*, Springer-Verlag, New York.
23. Freier, S. M., Kierzek, R., Jaeger, J. A., Sugimoto, N., Caruthers, M. H., Neilson, T., and Turner, D. H. (1986) *Proc. Natl. Acad. Sci. U.S.A. 83*, 9373−9377.
24. Serra, M. J., and Turner, D. H. (1995) *Methods Enzymol. 259*, 242−261.
25. Fedor, M. J., and Uhlenbeck, O. C. (1992) *Biochemistry 31*, 12042−12054.
26. Gumport, R. I., and Uhlenbeck, O. C. (1981) in *Gene Amplification and Analysis 2* (Chirikjian, J. G., and Papas, T. S., Eds.) p 314, Elsevier North-Holland, Inc., New York.
27. Dahm, S. C., Derrick, W. B., and Uhlenbeck, O. C. (1993) *Biochemistry 32*, 13040−13045.
28. Uhlenbeck, O. C. (1987) *Nature 328*, 596−600.
29. Sigurdsson, S. T., Tuschl, T., and Eckstein, F. (1995) *RNA 1*, 575−583.
30. Bassi, G. S., Murchie, A. I. H., and Lilley, D. M. (1996) *RNA 2*, 756−768.
31. Miller, W. A., and Silver, S. L. (1991) *Nucleic Acids Res. 19*, 5313−5320.
32. Miller, W. A., Hercus, T., Waterhouse, P. M., and Gerlach, W. L. (1991) *Virology 183*, 711−720.

BI980307Z